Article

Transition to the New Green Maritime Era—Developing Hybrid Ecological Fuels Using Methanol and Biodiesel—An Experimental Procedure

Dimitrios Parris [1],* , Konstantinos Spinthiropoulos [1] , Konstantinos Panitsidis [1] and Constantinos Tsanaktsidis [2]

[1] Department of Management Science and Technology, University of Western Macedonia, GR50100 Kozani, Greece; kspinthiropoulos@uowm.gr (K.S.); kpanytsidis@uowm.gr (K.P.)
[2] Department of Chemical Engineering, University of Western Macedonia, GR50100 Kozani, Greece; ktsanaktsidis@uowm.gr
* Correspondence: dimit.parris@gmail.com

Abstract: The conventional utilization of fossil fuels precipitates uncontrolled carbon dioxide and sulfur oxides emissions, thereby engendering pronounced atmospheric pollution and global health ramifications. Within the maritime domain, concerted global initiatives aspire to mitigate emissions by 2050, centering on the adaptation of engines, alteration of fuel compositions, and amelioration of exhaust gas treatment protocols. This investigation pioneers experimentation with marine gas oil augmented by methanol, a practice conventionally encumbered by prohibitively expensive additives. Successful amalgamation of methanol, animal-derived biodiesel, and marine gas oil (MGO) is empirically demonstrated under meticulously controlled thermal conditions, creating a homogeneous blend with virtually zero sulfur content and reduced carbon content, featuring characteristics akin to conventional marine gas oil but with no use of expensive emulsifiers. This new blend is suitable for employment in maritime engines utilizing Delaval technology, yet with significantly lower energy requirements compared to those necessitated using conventional very low sulfur fuel oil (VLSFO) with a maximum sulfur content of 0.5% *w/w*.

Keywords: methanol; diesel; biodiesel; FAME; marine fuel; fuel blend; GHG emissions; environmental protection

1. Introduction

International maritime transportation, a critical component of global commerce, is under pressure to improve energy efficiency and reduce carbon emissions [1]. The maritime industry is responsible for moving about 80–90% of global trade, transporting over 10 billion tons of cargo annually [2,3], contributing to 3% of total global greenhouse gas (GHG) emissions [4]. By 2019, global trade had grown by 18% since 2016, and shipping fuel consumption is projected to increase by 50% from 2012 to 2040 [5,6]. Heavy fuel oil (HFO), known for its high sulfur content, remains the dominant fuel in this sector [7].

The extensive conventional use of fossil fuels and emissions of the international commercial fleet have significantly contributed to environmental degradation, climate change, and the greenhouse effect. Up to 70% of these emissions have been detected within 400 km inland [8,9], impacting global health and sometimes leading to fatal diseases [9,10]. The global community is grappling with an energy crisis precipitated by the irreversible depletion of traditional fossil fuel reservoirs and the buildup of greenhouse gases in the atmosphere, leading to unprecedented shifts in weather patterns [11]. Ships' air emissions arise from complete fuel combustion, producing substances like carbon dioxide (CO_2) and sulfur oxides (SO_x), or from the oxidation of atmospheric nitrogen, resulting in nitrogen oxides (NO_x). Incomplete combustion generates pollutants such as hydrocarbons (HCs,

including methane (CH_4)), carbon monoxide (CO), formaldehyde, particulate matter (PM) including black carbon (BC) and polyaromatic hydrocarbons (PAHs), and particle number (PN) emissions. Some pollutants, such as nitrogen dioxide (NO_2), ammonia (NH_3), and nitrous oxide (N_2O), form during exhaust aftertreatment processes.

Heavy metals may also be emitted from fuel, lubricating oil, and engine wear [9]. SO_x and NO_x emissions impact both terrestrial and aquatic ecosystems through acid deposition and nutrient enrichment, leading to eutrophication [9].

Among greenhouse gases, CO_2 is the primary driver of global warming, with significant methane (CH_4) and nitrous oxide (N_2O) contributions, which have 100-year global warming potentials (GWP100) of 28 and 265 times that of CO_2, respectively. Another significant contributor to global warming is black carbon (BC), with a GWP100 of 900 [9,12].

In 2018, maritime activities emitted 1.06 gigatons (Gt) of CO_2 and other greenhouse gases globally, increasing 9.3% and 9.6% from 2012 levels, respectively. This accounts for approximately 2.89% of global anthropogenic CO_2 emissions, which rose to 3.0% by 2022 [7,9,13,14]. According to the European Maritime Safety Agency (EMSA), ships over 5000 gross tonnage (gt) within the EU consumed 44,132 metric megatons of fuel, resulting in 137.041 metric megatons of CO_2 emissions, excluding warships, fishing vessels, and auxiliary ships like tugboats [15].

The maritime sector faces urgent demands to limit or eliminate hazardous gas emissions. International organizations such as the International Maritime Organization (IMO), the US Environmental Protection Agency (EPA), and China's Ministry of Foreign Affairs and Climate Change have implemented measures to reduce emissions, aiming for a 40% reduction in sulfur oxides by 2030 and a 70% reduction in sulfur oxides and 50% reduction in GHG emissions, including CO_2, by 2050. Some proposals even target complete fuel neutralization by 2050, promoting new ecological fuels [1,7,16].

Enhancing efficiency through methods such as wind propulsion [17], optimizing shipping routes [18], and adopting slow steaming [19] can contribute to lowering fossil fuel use [20]. However, these improvements alone are insufficient to realize a complete (100%) reduction in emissions.

Thus, alternative fuels are essential to reduce operational vessels' emissions, allowing trade to continue while simultaneously lowering the sector's fossil fuel consumption. Utilizing low-carbon and renewable energy sources to meet shipping energy requirements is proposed as part of the approach to facilitate the sector's future energy transition [21]. Embracing low-carbon fuels will pose a multifaceted challenge, necessitating the creation of reliable supply chains, establishment of bunkering infrastructure, implementation of decarbonization policies, and introduction of economic mechanisms to support adoption [22]. The primary step, however, is to ensure that any alternative fuels employed can deliver a significant reduction in carbon emissions to achieve a complete (100%) reduction in GHG emissions by 2050 [17].

The European Union also emphasizes reducing gas emissions, particularly sulfur oxides, through European Directive EU 2016/802, mandating the use of very low sulfur fuel oil (VLSFO) with a maximum sulfur content of 0.5% w/w for all marine activities within the EU territory. Stricter measures apply to ships in European ports, anchorages, or Special Emission Control Areas (SECAs), where only marine gas oil (MGO) with a maximum sulfur content of 0.1% w/w is allowed. These limits came into force on 1 January 2020, replacing previous limits of 3.5% w/w for VLSFO and 1.0% w/w for MGO [23].

Internal combustion engines' SO_x emissions are reduced either by retention after fuel combustion using scrubbers or using fuels with low or zero sulfur content, as the emissions are proportional to the sulfur content in the fuel [9].

Research has focused on developing new eco-friendly fuels beyond conventional fossil fuels, aiming to reduce greenhouse gas emissions and promote resource sustainability. Among alternative fuels, methanol is a significant focus. In recent years, methanol has been a focal point for scientists, as it represents an alternative fuel with a high oxygen content. This characteristic enhances combustion in internal combustion engines and

reduces the emissions of hazardous gases [24]. Methanol has the simplest carbon structure, is nearly sulfur-free, and can be produced from renewable energy sources, such as direct CO_2 hydrogenation from the atmosphere [25].

It can be used as a fuel either through combustion or in fuel cells, producing carbon dioxide and water. Methanol derived from fossil fuels emits significant amounts of greenhouse gases when used in shipping. However, producing methanol through low-carbon or biogenic processes can reduce greenhouse gas emissions. Current commercial methanol production relies on fossil fuels and is characterized by high carbon emissions. In contrast, e-methanol (electro-methanol) is produced from green hydrogen and liquid carbon dioxide obtained from industrial processes. Kanchiralla et al. [26] examined the use of e-methanol as a marine fuel, where its production involves hydrogen from electrolysis and carbon dioxide captured directly from the air. This approach leads to net-zero greenhouse gas emissions during combustion, as the released carbon is sourced from the atmosphere and not from fossil reserves. The results indicate that e-methanol has very low greenhouse gas emissions, more than 80% lower than marine gas oil [26], and it is environmentally friendly and cost-effective [7,27,28]. Huang et al. [29] investigated e-methanol's production from renewable hydrogen and carbon dioxide collected from the exhaust gases of a fossil fuel power plant. The study attributes negative carbon credits to the used carbon dioxide, resulting in an 83% reduction in emissions compared to conventional fuels.

Methanol is currently produced on a large scale and can be easily integrated into existing infrastructure with minor modifications to marine engines and technology, primarily due to methanol's high corrosiveness and autoignition point [30–34].

Using methanol in internal combustion engines, typically in dual-fuel engines, results in minimal sulfur oxides and CO_2 emissions. The emitted sulfur oxides mainly come from engine lubricants or conventional petroleum used with methanol in dual-fuel engines [9].

Biofuels are fuels produced from biomass, which includes any organic matter derived from plants or animals. They serve as a renewable alternative to fossil fuels, offering potential for reducing greenhouse gas emissions and enhancing energy security [35]. They can reduce CO_2 emissions by sequestering CO_2 from the atmosphere during photosynthesis [36,37]. Biodiesel, derived from vegetable oils or animal fats through transesterification, can be used in internal combustion engines either as an additive or primary fuel, similar to conventional diesel. When methanol is used for the reaction, it results in fatty acid methyl esters (FAME) [38–40]. Biodiesel reduces gas emissions and complies with International Maritime Organization requirements [1,41].

Biodiesel can be obtained from biomass, which in turn can be used as fuel. Biodiesel is combined with fossil diesel for commercial use [42]. Biodiesel is a renewable and biodegradable resource with a lower sulfur content, higher cetane number, greater efficiency, and better lubricant properties [43], thus making it superior to its fossil diesel counterpart [44].

Biodiesel derived from renewable resources is emerging as a highly appealing alternative fuel due to its minimal emissions and favorable chemical properties, including non-toxicity, biodegradability [45], and carbon neutrality [46]. Furthermore, biodiesel can be utilized in standard diesel engines, unlike fossil-based fuels (petroleum or diesel). Fossil fuels are finite and release various pollutants such as nitrogen oxides, sulfur oxides, carbon oxides, lead, and hydrocarbons [47,48].

The predominant and most efficient method for biodiesel synthesis is transesterification, also known as methanolysis [49]. This process involves a catalytic reaction where vegetable oil reacts with alcohol, resulting in the formation of biodiesel and glycerol [50,51]. During transesterification, the glycerol moiety in triglycerides is substituted with a short-chain alcohol [52]. The reaction proceeds through a series of three successive and reversible steps: triglycerides are first converted into diglycerides, which are then transformed into monoglycerides, and finally, monoglycerides are converted into glycerol. Each stage of the process generates an ester, ultimately producing three ester molecules from one triglyceride molecule [48,53].

Extensive studies and prior research indicate that biodiesel synthesis via transesterification can be facilitated by both homogeneous catalysts (acids and bases) and heterogeneous

catalysts (acids, bases, and enzymes) [54]. However, transesterification processes employing acid and alkali catalysts are demonstrated to be more time-efficient and cost-effective compared to enzyme-catalyzed methods. In this process, a catalyst breaks down the oil molecules, and an alcohol (such as ethanol or methanol) reacts with an ester to form an alkyl ester (either ethyl or methyl) [48].

Marine internal combustion engines using methanol–diesel employ three methods: port injection, in-cylinder direct injection (requiring dual-fuel engines), and direct mixing. Direct mixing, however, requires expensive additives or emulsifiers due to the differing properties of diesel and methanol [25].

Current research focuses on three areas to reduce harmful gas emissions: engine modifications, after-combustion treatment technologies, and fuel modifications [10]. This study focuses on fuel modification, aiming to create a homogeneous methanol–marine gas oil (MGO) blend without costly chemical additives, determining optimal conditions and proportions for the blend, and comparing its characteristics with conventional marine fuel.

2. Materials and Methods

The experiment was conducted at the Laboratory of Environmental Technology, Department of Chemical Engineering, School of Engineering, University of Western Macedonia, Greece.

During the experimental procedure, attempts were made to determine the maximum methanol (MeOH) content that can be dissolved in (MGO) with a maximum sulfur content (S) of 0.1% w/w, in the presence of animal (FAME) and vegetable biodiesel without the addition of emulsifiers or other expensive additives. Subsequently, an attempt was made to determine the lowest temperature at which mixing could occur without loss of any of the components, and finally to calculate the minimum time required for the three materials to mix into a uniform transparent mixture, attempting also to determine if a mixing-specific method, other than direct mixing of the materials, could optimize blending of the three components.

The current research reveals that the maximum ratio of methanol that can be used in diesel blends with the aid of stabilizers, such as butanol, is 20% [55,56]. In the present study, given that the maximum methanol content was investigated without the addition of extra stabilizers but only with the presence of biodiesel, the experimental procedure commenced with a much lower methanol ratio. A ratio of MGO 95%–methanol 5% was selected, and the quantities were adjusted, always maintaining the methanol–biodiesel ratio at 1:2 by volume. This approach is in accordance with previous research findings, which indicate that this ratio achieves the most effective dissolution of methanol in the biofuel [57].

The starting temperature for the experiment was set at 15 °C (room temperature). Depending on the behavior of the mixtures under testing, the temperature was gradually increased until the minimum temperature at which the materials achieved mixing was identified.

For the experimental procedure, MGO (S = 0.090 wt%) was utilized, determined using the ISO 20884:2019 [58] method. The sample's density (d) was measured at 0.8353 g/mL at 25 °C according to the EN ISO 12185:1996 [59] method, its kinematic viscosity (Visc) at 40 °C was determined to be 2.9912 cSt using the EN ISO 3104:2020 [60] method, its calorific value was assessed at 45,919 J/g by the ASTM D240-19 [61] method, and the electrical conductivity was measured at 3 pS. The MGO's characteristics are shown in Table 1 below.

Table 1. MGO's characteristics.

Parameter	Method	Measurement
Density (25 °C)	EN ISO 12185:1996 [59]	0.8353 gr/mL
Kinematic Viscosity (40 °C)	EN ISO 3104:2020 [60]	2.9912 cSt
Heat-producing Energy	ASTM D240-19 [61]	45,919 J/gr
Sulfur (S)	ISO 20884:2019 [58]	0.090 w/w
HC Containing: C_{10}–C_{40}	ISO 17025:2017 (GC-FID) [62]	94% w/w
MeOH Containing	ISO 17025:2017 (HPLC-RI) [62]	00.0 w/w
Electrical Conductivity	ASTM D2624-22 [63]	3 pS

Animal biodiesel (FAME) with a sulfur content of 5.2 mg/kg, measured using the EN ISO 20846 [64] method, was employed as the second component. The sample's density (d) was determined to be 0.8757 g/mL using the EN ISO 12185 method at 15 °C. Its flash point was measured at 174 °C according to the EN ISO 3679 [65] method. The cloud point was found to be at 12 °C using the EN 23015 [66] method, with a water content of 130 mg/kg determined by the EN ISO 12937 [67] method. The acidity was recorded at 0.17 mg KOH/g via the EN 14104 [68] method. The ester content measured greater than 99% m/m by the EN 14103 [69] method, with linolenic acid methyl ester at 0.9 m/m by the same method, and polyunsaturated methyl esters (≥4 double bonds) at <0.5% m/m by the EN 15779 [70] method. Animal derived biodiesel's characteristics are shown in the Table 2 below.

Table 2. Animal-derived biodiesel's characteristics.

Parameter	Method	Measurement
Density (15 °C)	EN ISO 12185 [59]	0.8757 g/mL
Flash point	EN ISO 3679 [65]	174 °C
Cloud point	EN 23015 [66]	12 °C
Acidity	EN 14104 [68]	0.17 mg KOH/g
Ester Content	EN 14103 [69]	<99% m/m
Linolenic acid methyl ester	EN 14103 [69]	0.9 m/m
Polyunsaturated methyl esters (≥4 double bonds)	EN 15779 [70]	<0.5% m/m
Sulfur (S)	EN ISO 20846 [64]	5.2 mg/kg

As a third component, pure commercial methanol with a content of 100% was utilized, having a density (d) of 0.79 kg/L, a boiling point of 64 °C, a water content of 0.01%, and an electrical conductivity exceeding 2000 pS.

To determine the content of C_{10}–C_{40} hydrocarbons in the final blends, chromatography was conducted employing the gas chromatography—flame ionization detection (GC–FID) method. Additionally, for the methanol (MeOH) content in the final blends, chromatography was conducted using the high-performance liquid chromatography refractive index (HPLC-RI) method. These analyses were performed in a laboratory certified according to ISO 17025:2017 [62].

The measurement of total petroleum hydrocarbons (TPH) was conducted using the GC–FID method on an Agilent brand device, model 8890 GC–FID, manufactured in the United States of America. The procedure involved extraction with hexane and injection into the GC–FID chromatograph using a 30-m HP-5 column. The chromatographic conditions were as follows: Inlet module PTV in splitless mode, injection volume 1 µL, baffled liner PTV, 2.0 mm × 2.75 mm × 120 mm, inlet temperature 50 °C, hydrogen gas carrier; carrier gas flow at 3.2 mL/min in a constant flow, split flow at 50 mL/min, splitless time at 0.5 min, and septum purge flow at 5 mL/min.

The measurement of methanol was conducted using the HPLC-RI method on a Thermo brand device, model HPLC UltiMate 3000, manufactured by ThermoFisher Scientific in Germany. The procedure involved extraction with ultrapure water and injection into the HPLC-RI chromatograph using a 5 µm UniverSil HS C18 column. The chromatographic conditions were as follows: flow rate at 0.6mL min^{-1}, injection volume of 20.0 µL, column oven and detector temperature at 30 °C, and 8.0 min for total run Mobile phase, and samples were filtered before injection using 0.2 µm polytetrafluoroethylene (PTFE) membrane filter (Millipore, Bedford, PA, USA).

The final mixture's viscosity was measured using a Viscosimetro SCHOTT brand device, model CT 52, manufactured by SCHOTT Instruments GmbH, in Mainz, Germany, the calorific power using an IKA brand device, model C200 meter manufactured by IKA-Werke GmbH & Co. KG, in Staufen, Germany, and the density using a Precisa brand device, model XT20A, manufactured in Precisa Gravimetrics AG, in Dietikon, Switzerland.

2.1. Experiment 1

According to the experimental procedure, the optimal ratio of methanol to biodiesel was considered to be 1:2 [57]. A mixture was created at a ratio of 5% methanol to 10%

plant-derived biodiesel and 85% marine gas oil (MGO) with a maximum sulfur content of 0.1% w/w, as shown in Table 3 below.

Table 3. Percentages % v/v of component ratios in plant-derived biodiesel-added blends.

% v/v	Blend 1	Blend 2	Blend 3	Blend 4	Blend 5
Methanol	5	10	15	20	25
Bio. (Plant)	10	20	30	40	50
MGO	85	70	55	40	25
Temp. °C					
15–25	No result	No result	No result	No result	No result
25	No result	No result	No result	No result	No result
25–59	No result	No result	No result	No result	No result
59	No result	No result	No result	No result	No result
>60 °C	MeOH Evapor.	MeOH Evapor.	MeOH Evapor.	MeOH Evapor.	MeOH Evapor.

The same procedure was carried out using animal-derived biodiesel (FAME).

Each mixture was gradually heated with agitation at regular time intervals starting from a room temperature of 15 °C, in which no mixing occurred. It was observed that at a temperature of 25 °C, the mixing process commenced in the animal-derived biodiesel blends, whereas at a temperature of 59 °C, precisely 5 °C lower than the boiling point of methanol and 1 °C lower than the flash point of marine gas oil (MGO) with a maximum sulfur content of 0.1% w/w, a homogeneous transparent mixture was achieved.

The same procedure was repeated with each doubling of the quantity of methanol and animal-derived biodiesel, while maintaining a constant ratio of 1:2 and decreasing the content of marine gas oil. In this manner, mixtures were created using animal-derived biodiesel (FAME) in proportions detailed in the following Table 4.

Table 4. Percentages % v/v of component ratios in FAME-added blends.

% v/v	Blend 1	Blend 2	Blend 3	Blend 4	Blend 5
Methanol	5	10	15	20	25
Bio. (FAME)	10	20	30	40	50
MGO	85	70	55	40	25
Temp. °C					
15–25	No result	No result	No result	No result	No result
25	Start Mixing	Start Mixing	Start Mixing	Start Mixing	No result
25–59	Mixing	Mixing	Mixing	Mixing	No result
59	Clear Blend	Clear Blend	Clear Blend	Clear Blend	No result
>59 °C	MeOH Evapor.	MeOH Evapor.	MeOH Evapor.	MeOH Evapor.	MeOH Evapor.

Mixtures using plant-derived biodiesel in different proportions are outlined in the following Table 3.

Regarding the blends in Table 4, it was observed that up to blend ratio 4 (methanol 20% v/v–animal-derived biodiesel 40% v/v–MGO 40% v/v), mixing was achieved at a temperature of 55°C. However, for mixture ratio 5 in Table 4 (methanol 25% v/v–animal-derived biodiesel 50% v/v–MGO 25% v/v), no mixing of the materials occurred. The temperature gradually increased, but without success, as it approached the boiling point of methanol, resulting in its evaporation. For this reason, mixture 4 from Table 4 (methanol 20% v/v–animal-derived biodiesel 40% v/v–MGO 40% v/v) was re-prepared, with an increase in the methanol's content and animal biodiesel (FAME) by 0.5 mL each time, while maintaining the ratio constant and accordingly reducing the marine fuel's content. As a result, mixtures were prepared as listed in Table 5.

Table 5. Exact proportions % *v/v* of blend components with added FAME.

% *v/v*	Blend 6	Blend 7	Blend 8	Blend 9
Methanol	20.5	21	21.5	22
Bio. (Fame)	41	42	43	44
MGO	38.5	37	35.5	34
Temp. °C				
15–25	No result	No result	No result	No result
25	Start Mixing	Start Mixing	Start Mixing	No result
25–59	Mixing	Mixing	Mixing	No result
59	Clear Blend	Clear Blend	Clear Blend	No result
>59 °C	MeOH Evapor.	MeOH Evapor.	MeOH Evapor.	MeOH Evapor.

It was found that the maximum possible ratio for dissolution at a temperature of 55 °C was that described in blend 8 of Table 5 (methanol 21.5% *v/v*–animal-derived biodiesel 43% *v/v*–MGO 35.5% *v/v*). Further increases in the methanol's content and proportions did not result in mixing. It was also observed that at every mixture ratio with added plant biodiesel, mixing was not achieved. For this reason, plant biodiesel's use was rejected.

For this reason, it is considered that the maximum blending ratio of methanol—animal biodiesel (FAME)—marine fuel is 21.5% *v/v*–43% *v/v*–35.5% *v/v*.

Maintaining the aforementioned observation, the experimental procedure continued to determine the lowest temperature at which material mixing could occur, as well as whether the outcome was affected by gradual or simultaneous mixing of the materials.

2.2. Experiment 2

A 35.5 mL volume of marine gas oil (MGO) quantity with a maximum sulfur content of 0.1% *w/w*, 5 mL of methanol, and 10 mL of animal biodiesel (FAME) were placed in a container at room temperature (15 °C). The mixture was gradually heated on a heated base with a stirrer. The mixing process commenced at 25 °C, and at a temperature of 59 °C and above, a clear, transparent mixture was achieved.

At this point, an additional 5 mL of methanol and 10 mL of animal biodiesel (FAME) were added. The new mixture immediately separated upon contact with the already uniform mixture, while the temperature of the preheated mixture decreased. Maintaining the heating, new mixing occurred again when the temperature approached 59 °C. The process was repeated until the final ratio of components was achieved, as described in Table 5 for blend 8 of the first experiment (methanol 21.5% *v/v*–animal-derived biodiesel 43% *v/v*–MGO 35.5% *v/v*). The procedure is shown in Table 6 below.

Table 6. Gradual mixing procedure of materials.

Blend (MeOH–Fame–MGO) Volume Units	15 °C–25 °C	25 °C	25 °C–59 °C	59 °C	Add Methanol–Fame Volume Units	Temp. Decreased	59 °C
5–10–35.5	No Result	Start Mix.	Mixing	Blend	5–10	Separation	Blend
10–20–35.5	No Result	Start Mix.	Mixing	Blend	5–10	Separation	Blend
15–30–35.5	No Result	Start Mix.	Mixing	Blend	5–10	Separation	Blend
20–40–35.5	No Result	Start Mix.	Mixing	Blend	0.5–1.0	Separation	Blend
20.5–41–35.5	No Result	Start Mix.	Mixing	Blend	0.5–1.0	Separation	Blend
21–42–35.5	No Result	Start Mix.	Mixing	Blend	0.5–1.0	Separation	Blend
21.5–43–35.5	No Result	Start Mix.	Mixing	Blend	0.5–1.0	Separation	Blend
22–44–34	No Result	No Result	No Result	No Result	-	-	-

2.3. Experiment 3

The materials were placed in a container in the proportions described in the first experiment's Table 5 for blend 8 (methanol 21.5% *v/v*–animal-derived biodiesel 43% *v/v*–MGO 35.5% *v/v*) and at room temperature of 15 °C, and heated on a heated base with a stirrer. In this case, the mixing process commenced again at 25 °C, while the mixture homogenized at a temperature of 58 °C instead of the previous 59 °C. The procedure is shown in Table 7 below.

Table 7. Direct mixing of materials heated on a heated base procedure.

Blend (Methanol–Fame–MGO%) *v/v*	Temperature					
	15 °C–25 °C	25 °C	25 °C–58 °C	58 °C	59 °C	60 °C
21.5–43–35.5	No Result	Start Mix.	Mixing	Blend	Blend	Start Evaporation

In the next phase, an attempt was made to determine the behavior of the materials when uniformly heated separately before mixing, as well as the minimum temperature and time required for mixing.

2.4. Experiment 4

An amount of the 3 materials was placed in three separate containers, which were heated uniformly throughout their entire bodies simultaneously in a thermostatic bath. The temperature selected for the initial examination was 25 °C at which, according to previous tests, the mixing process was observed to commence.

When the 3 materials reached a temperature of 25 °C, material was taken from each container according to experiment 1 of blend 8, Table 5 ratio (methanol 21.5% *v/v*–animal-derived biodiesel 43% *v/v*–MGO 35.5% *v/v*), and the three quantities were mixed in a common container. The materials separated immediately. The experiment proceeded by extending the materials' dwell time at a temperature of 25 °C for 5 min, after which the materials were mixed again at the desired ratio, resulting once again in complete separation.

The same procedure was repeated several times, increasing the time by 5 min each time while maintaining a constant temperature of 25 °C, until the materials remained heated separately for 2 h or more. In each case, mixing was not achieved.

The process was repeated from the beginning with a 5 °C temperature increase. Even at a temperature of 30 °C, mixing was still not achieved over time.

The experiment was repeated multiple times until it was observed that at a temperature of 49 °C the mixing procedure started; at the temperature of 55 °C, following separate materials' heating for one hour, the materials were mixed into a turbid mixture. The same procedure continued without a difference in the outcome, and the mixture remained turbid, while due to approaching the boiling temperature of the alcohol, loss of material was observed due to evaporation after one hour or more of heating.

Subsequently, the turbid mixture, which was at a temperature of 55 °C with heating for one hour, was uniformly placed in the water bath. It was observed that after 45 min, the mixture became clear and transparent.

Subsequently, it was allowed to cool, and it was observed that phase separation began at 51 °C while the mixture fully separated at a temperature lower than 49 °C.

After reheating, it was observed that the mixture homogenized into a clear and transparent state at a temperature of 52 °C, which is 3 °C lower than the initial temperature.

The process was repeated several times; however, the temperature for complete mixing remained consistently at 52 °C.

The mixing process and the materials' phases at each temperature level are detailed more analytically below.

The 3 materials were heated uniformly in three separate containers throughout their entire bodies simultaneously in a thermostatic bath at 25 °C, as shown in Figure 1 below.
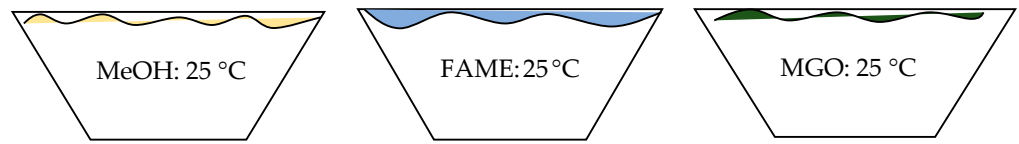
Figure 1. Separate uniform heating of the 3 materials at 25 °C.

An effort to create a homogeneous mixture from the three materials was made.

A.   Extending the materials' dwell time at a temperature of 25 °C for 5 min.

A new mixture, methanol 21.5% *v/v*–animal-derived biodiesel (FAME) 43% *v/v*–MGO 35.5% *v/v* was taken every 5 min, up to 2 h. Mixing was not achieved.

B.   Increasing gradually the 3 materials' temperature by 5 °C and taking a new mixture for every new trial to the same ratio as above.

The seperated, uniform, materials' heating progress, is shown in Figure 2 below.
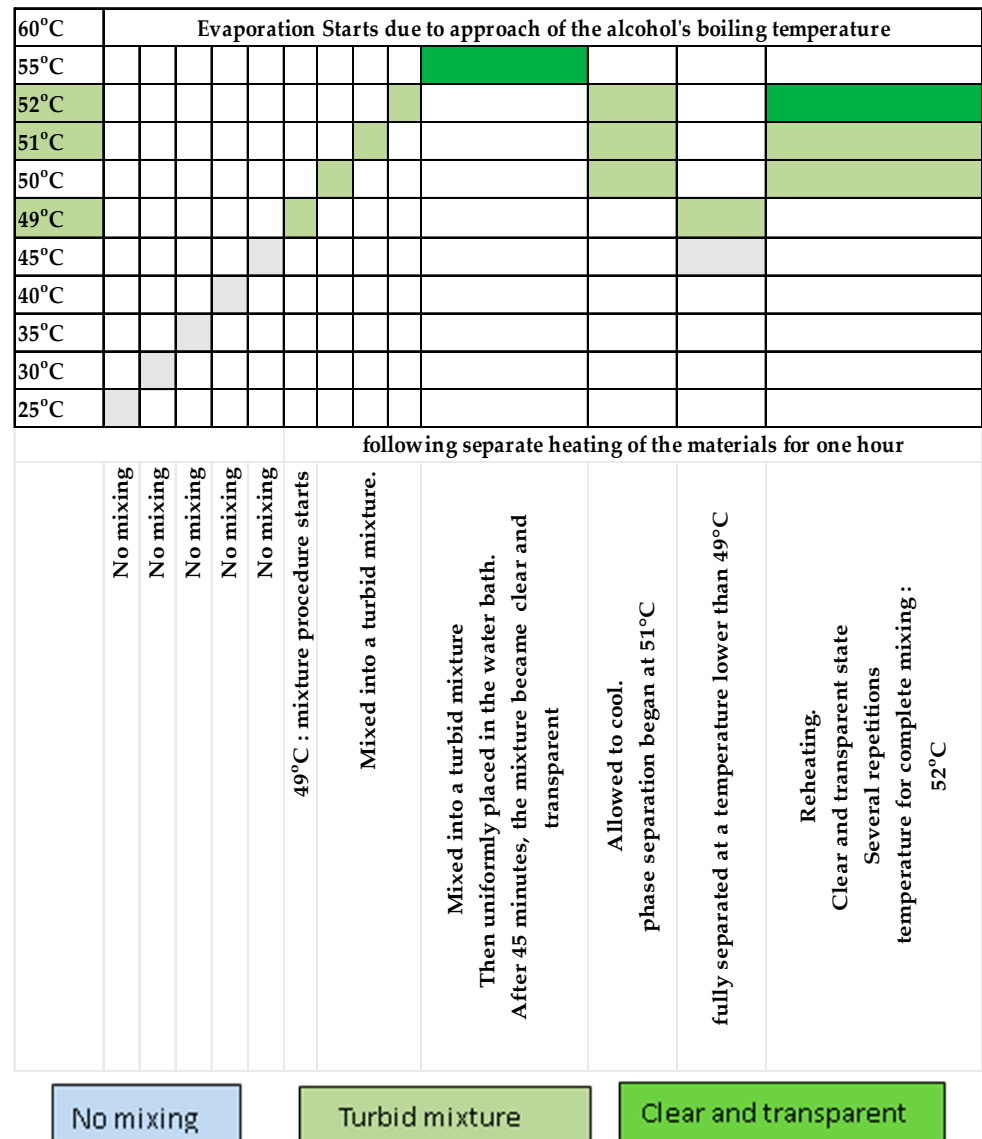

						49°C: mixture procedure starts	Mixed into a turbid mixture.	Mixed into a turbid mixture / Then uniformly placed in the water bath. / After 45 minutes, the mixture became clear and transparent	Allowed to cool. / phase separation began at 51°C	fully separated at a temperature lower than 49°C	Reheating. / Clear and transparent state / Several repetitions / temperature for complete mixing: 52°C
60°C	Evaporation Starts due to approach of the alcohol's boiling temperature										
55°C							Clear and transparent				
52°C								Clear and transparent	Clear and transparent		Clear and transparent
51°C								Turbid	Turbid		Turbid
50°C							Turbid		Turbid		Turbid
49°C						Turbid				Turbid	
45°C					No mixing					No mixing	
40°C				No mixing							
35°C			No mixing								
30°C		No mixing									
25°C	No mixing										

following separate heating of the materials for one hour

Legend: No mixing | Turbid mixture | Clear and transparent

Figure 2. Separate uniform heating of materials.

3. Results

As described in the previous chapter, the experimental procedure was conducted in the Laboratory of Environmental Technology at the Department of Chemical Engineering of the School of Engineering at the University of Western Macedonia and relied on the multiple trials method with observation. The measurements were carried out both in the same laboratory and in a secondary external accredited laboratory according to ISO 17025:2017 [62].

For the experiment, marine gas oil (MGO) with a maximum sulfur content of $S \leq 0.1\%$ *w/w*, animal-derived biodiesel (FAME), vegetable-derived biodiesel, and commercially available anhydrous methanol at 100% purity were used.

The physicochemical properties of methanol [71], the animal-derived biodiesel's characteristics according to the European standard EN 14214 [72], the marine fuel specifications according to ISO 8217:2017 [73], and chemical analyses' tables of the three materials utilized are presented in Appendix A.

From the experimental process, it emerged that there was an inability to blend methanol and MGO using vegetable-derived biodiesel. For this reason, this particular material was excluded from further processing.

It was observed that in a 100% *v/v* blend unit, the methanol's maximum quantity, capable of dissolving in MGO in the presence of animal-derived biodiesel (FAME), is 21.5% *v/v*. The remaining proportions correspond to MGO 35.5% *v/v* and FAME 43% *v/v*.

During the tests, three blends were obtained. The first was created by continuously and simultaneously heating the materials on a heated base and gradually adding methanol and biodiesel to each mixture. The second involved simultaneously mixing all materials and heating on a heated base, while the third involved heating the materials individually throughout their entire volume using a heat bath, followed by their consolidation and reheating in the total volume of the mixture, uniformly within a heat bath.

3.1. Results of the First Incremental Addition Blend

During the first incremental addition blend's preparation, it was observed that the homogenization process initiated at 25 °C, while complete mixing into a uniform and transparent mixture occurred at a temperature of 59 °C and above.

This method requires elevated temperature due to the continuous addition of materials and the mixture's temperature decrease, resulting in the loss of methanol and hydrocarbons to an extent that renders the blend unsuitable for preparation in an industrial scale.

As revealed by the final blend's measurement, the hydrocarbons' C_{10}–C_{40} content significantly decreased, with only 28.4% remaining, while the blend's methanol content decreased even further, with a final residual quantity of 9% of the initial amount.

However, a significant reduction in the blend's sulfur content was observed, as it decreased by approximately 90%, with a final content of only 0.01% *w/w* of the mixture.

The blend's calorific value reached 40,871 J/g, the density (d) was at 0.8548 g/mL, and the kinematic viscosity at 40 °C was 2.9616 cSt.

The final mixture's hydrocarbon content is depicted in Figure 3 below.

The mixture's final methanol content is depicted in Figure 4 below.

The final incremental addition blend's characteristics are presented in the following Table 8.

Table 8. Gradual addition blend's characteristics.

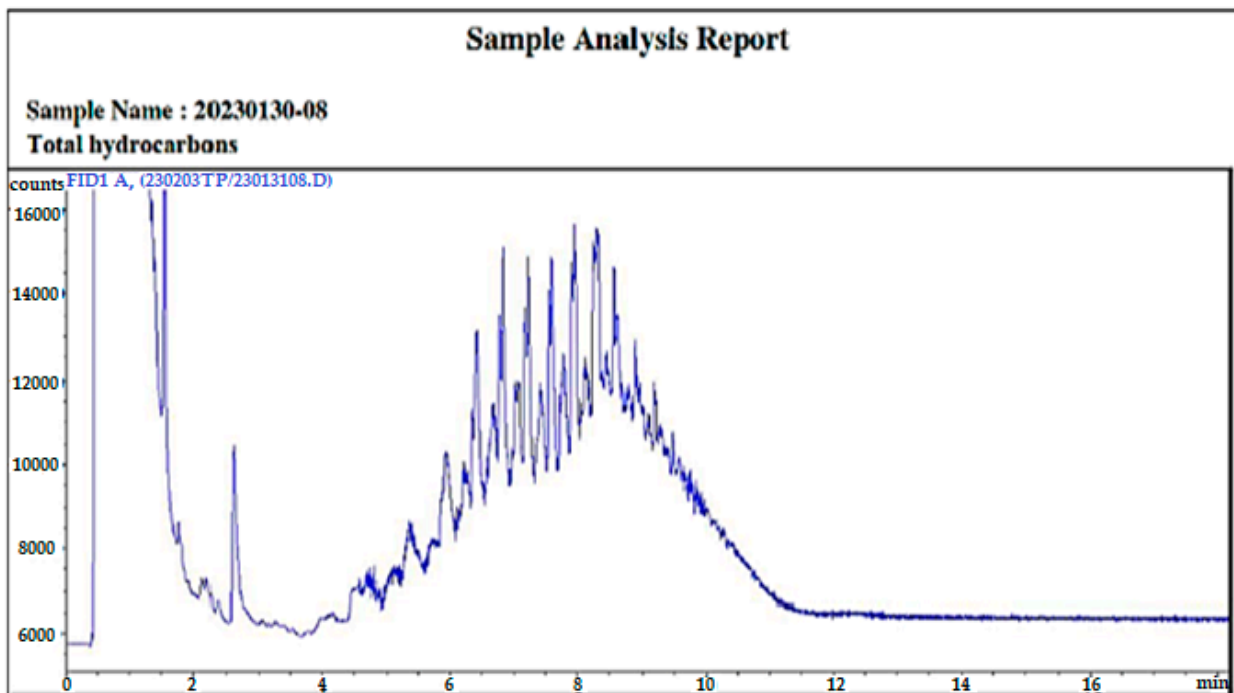| Parameter	Measurement
Density	0.8548 gr/mL
Kinematic Viscosity (40 °C)	2.9616 cst
Heat-producing Energy	40,871 j/gr
Sulfur (S)	0.01% *w/w*
HC Containing C_{10}–C_{40}	28.4% *w/w*
MeOH Content	9% *w/w*
Electrical Conductivity	>2000

Figure 3. Final hydrocarbon content in the incremental addition blend mixture.
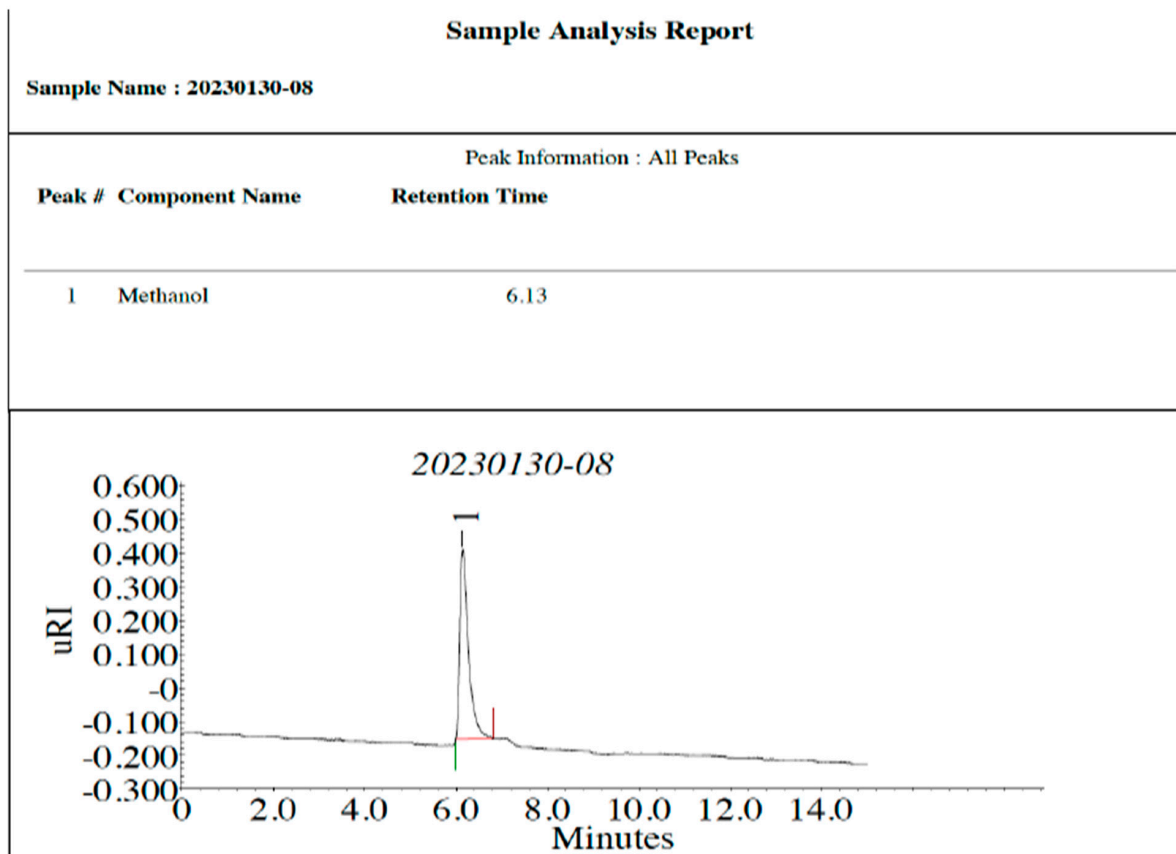

Figure 4. Final content in the incremental addition blend mixture.

3.2. Results of the Second Direct Blending Mixture

During the second simultaneous blending mixture preparation, it was observed that the homogenization process initiates at 25 °C, while complete mixing into a uniform and

transparent mixture occurs at a temperature of 58 °C and above, which is one degree lower than the temperature of the incremental blending process.

Due to the mixture's volume, this method requires prolonged exposure of the mixture to the heated device in order to reach the required temperature, resulting in a greater loss of methanol compared to that of the incremental blending process, as well as hydrocarbons. Consequently, this particular process becomes impractical for mixing the materials.

As evidenced by the final blend's measurement, the C_{10}–C_{40} hydrocarbons' content decreased significantly, with only 32.1% remaining, while the blend's methanol content decreased even further, with a final residual quantity of 7.2% of the initial amount.

However, a significant sulfur content decrease was observed for the blend, as it decreased by approximately 90%, with a final content of only 0.0103% *w/w* of the mixture.

The blend's calorific value reached 40,919 J/g, the density (d) was at 0.8412 g/mL, and the kinematic viscosity at 40 °C was 3.3318 cSt.

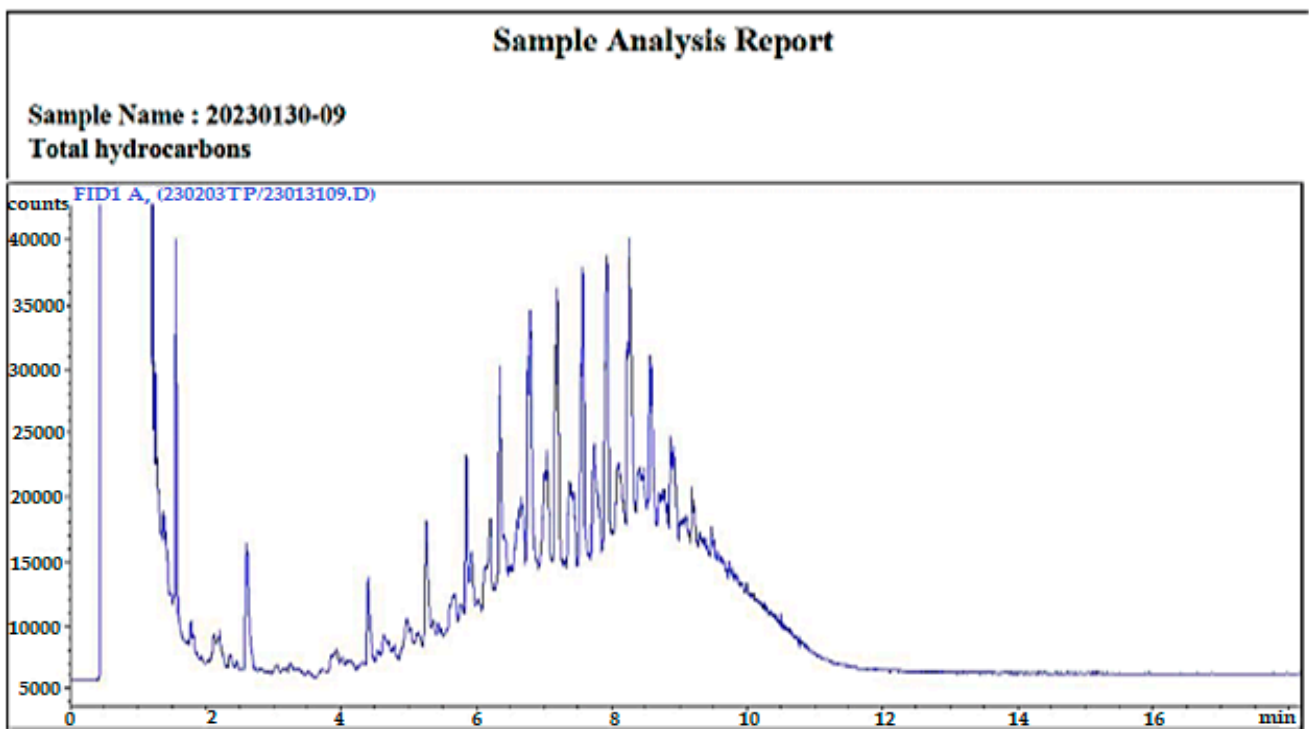The final blend's hydrocarbon content is depicted in Figure 5 below.

Figure 5. Final hydrocarbon content in direct blending of materials.

The final blend's methanol content is depicted in Figure 6 below.

The characteristics of the final simultaneous addition blend mixture are provided in the following Table 9.

Table 9. Direct mixture blend's characteristics.

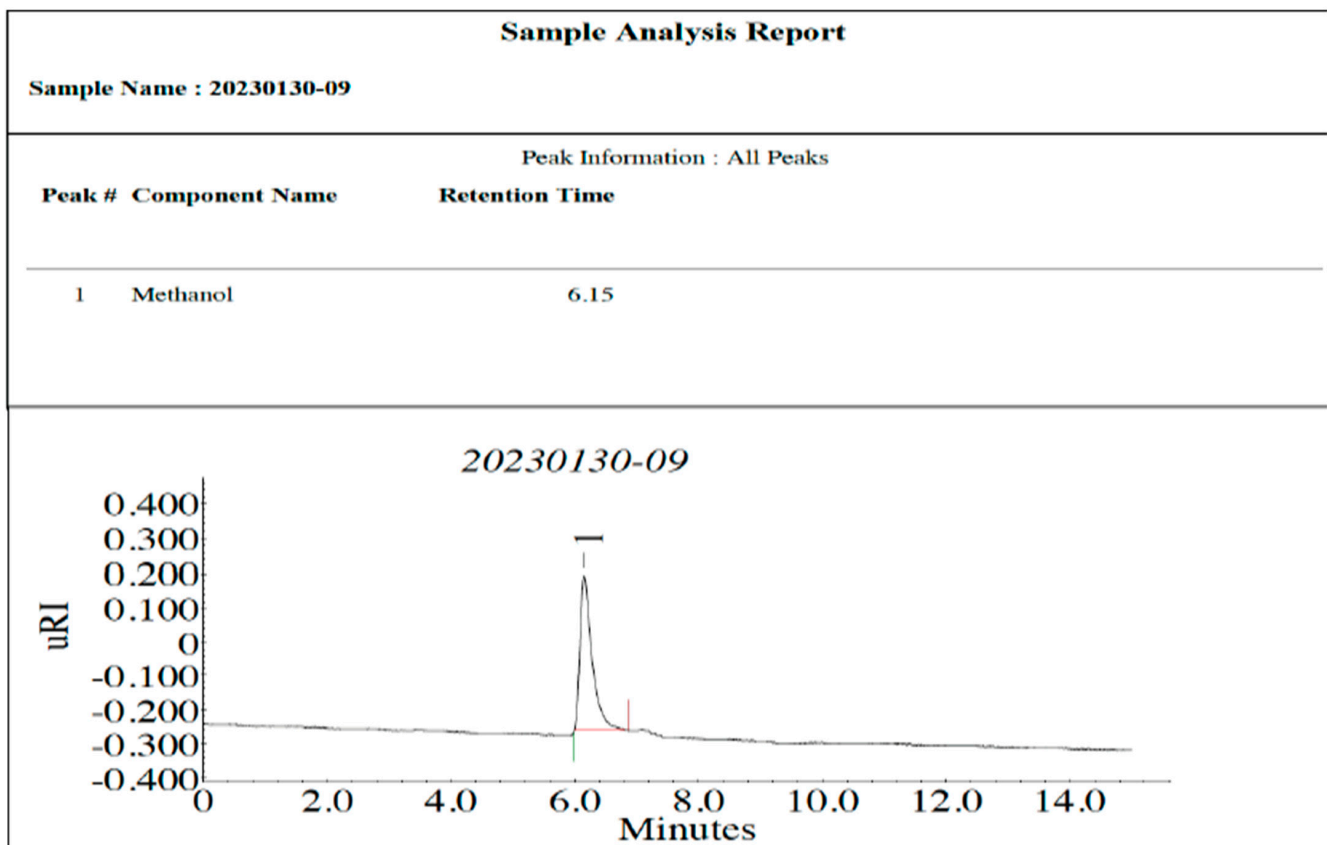| Parameter	Measurement
Density	0.8412 gr/mL
Kinematic Viscosity (40 °C)	3.3318 cst
Heat-producing Energy	40,919 j/gr
Sulfur (S)	0.0103% *w/w*
HC Containing C_{10}–C_{40}	32.1% *w/w*
MeOH Content	7.2% *w/w*
Electrical Conductivity	>2000

Figure 6. Final methanol content in direct blending of materials.

3.3. Results of the Third's Separate Heating Materials' Blend

During the third blend's preparation of heating the materials separately, it was observed that the homogenization process initiated at 49 °C, while complete mixing into a uniform and transparent mixture occurred at a temperature of 55 °C and above.

This method requires prolonged exposure of the mixture to uniform heating, following separate heating of the materials. Due to the relatively low temperature throughout the mixture's volume, blending of the materials was observed without significant loss through evaporation. Consequently, the materials appeared in the final blend with a content that nearly approached 100% of their quantities before processing.

As revealed by the final blend's measurement, the C_{10}–C_{40} hydrocarbons' content decreased minimally with a retention of 34.2% compared to the initial quantity corresponding to 35.5%. Methanol also decreased slightly, with a content of 20.2% of the initial quantity corresponding to 21% *v/v* of the mixture.

The sulfur content remained almost negligible, at a rate of 0.0104% *w/w* of the initial mixture.

The blend's calorific value reached 38,746 J/g, the density (d) was at 0.8423 g/mL, and the kinematic viscosity at 40 °C was 2.9319 cSt.

A significant observation is the temperature of 52 °C, at which the mixture homogenized after separation and remained uniform and transparent without loss of its constituents.

The final hydrocarbon content in the mixture is depicted in Figure 7 below.

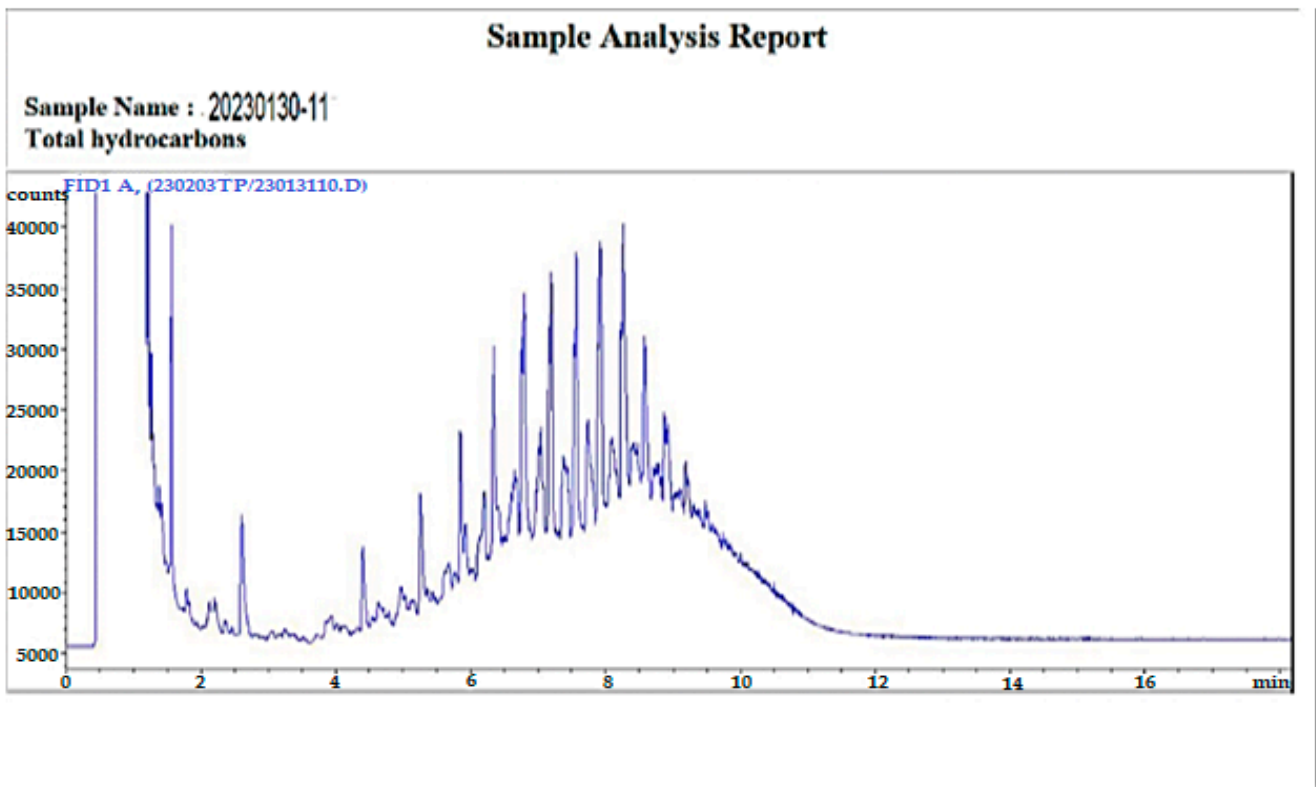The final methanol's content in the mixture is depicted in Figure 8 below.

Figure 7. Final hydrocarbon content in the blend after heating materials separately.
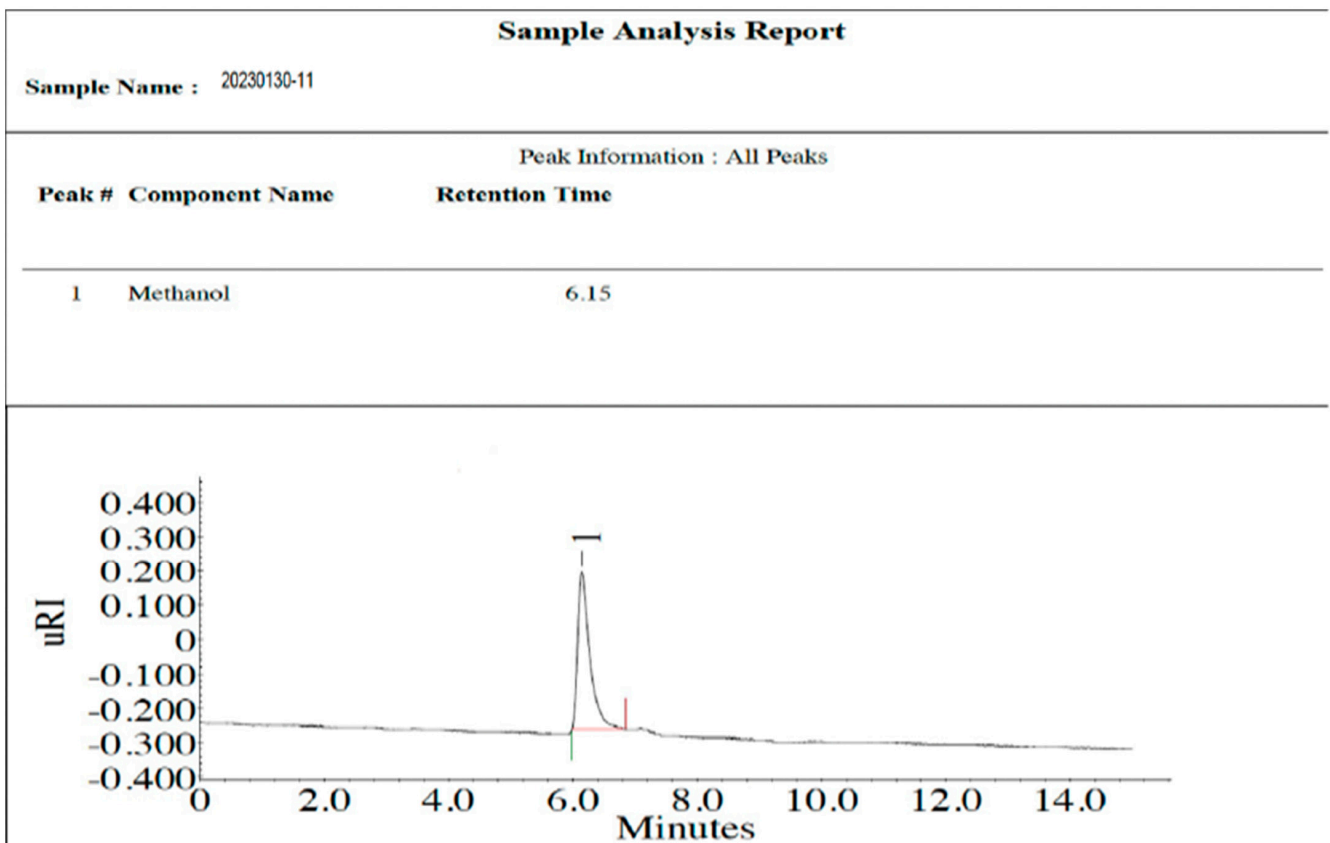

Figure 8. Final methanol content in the blend after heating materials separately.

The final blend's characteristics with simultaneous additions of components are presented in the following Table 10.

Table 10. Characteristics of separated heated materials' blend.

Parameter	Measurement
Density	0.8423 gr/mL
Kinematic Viscosity (40 °C)	2.9319 cst
Heat-producing Energy	38,746 j/gr
Sulfur (S)	0.0104% w/w
HC Containing C_{10}–C_{40}	34.2% w/w
MeOH Content	20.2% w/w
Electrical Conductivity	>2000

The three final blends' characteristics are presented collectively in Table 11 below.

Table 11. Final three blends' characteristics and behavior.

Parameter	Gradual Prepar.	Direct Mixture	Separated Material's Heating
Content % v/v in MeOH–FAME–MGO	21.5–43–35.5	21.5–43–35.5	21.5–43–35.5
Density	0.8548 gr/mL	0.8412 gr/mL	0.8423 gr/mL
Kinematic Visc. (40 °C)	2.9616 cst	3.3318 cst	2.9319 cst
Heat-producing Energy	40,871 j/gr	40,919 j/gr	38,746 j/gr
Sulfur (S)	0.01% w/w	0.0103% w/w	0.0104% w/w
HC Containing C_{10}–C_{40}	28.4% w/w	32.1% w/w	34.2% w/w
MeOH Content	9% w/w	7.2% w/w	20.2% w/w
Electrical Conductivity	>2000	>2000	>2000
Temperature °C			
15–25	No Result	No Result	
25	Start Mixing	Start Mixing	
25–49			No Result
25–58		Mixing	
25–59	Mixing		
49			Start Mixing
50–54			Mixed into Turbid Mixture
55			Clear and transparent after 45 min at this temp.
58		Clear Blend	
59	Clear Blend		
55–60			Clear and transparent after 45 min at this temp.
58–60		Blend	
59–60	Blend		
>60	Start Evapor.	Start Evapor.	Clear and transparent after 45 min at this temp.
After Cooling			
51			Start Separation Procedure
49			Fully Separated
After Reheating			
52			Immediately clear and transparent blend

4. Discussion

As evidenced by the experimental procedure, a homogeneous and transparent mixture of MGO and methanol can be achieved in the presence of animal biodiesel (FAME) additive and maintained in this state at a temperature of 52 °C, without the need for emusifiers or other expensive additives. Animal biodiesel was chosen as an additive due to its increased content of fatty acids (polar carboxyl groups).

The process's initial phase is based on the principle of "like dissolves like". The three materials consist of hydrocarbons, although MGO constitutes a nonpolar compound while methanol is polar. The hydroxide radicals of the methanol molecules strongly bind to one another, making it impossible for direct dissolution in the diesel molecules.

However, due to the animal biodiesel's participation, which contains polar carboxyl groups, the interaction of methanol's polar groups with the fatty acids (polar group OH) becomes feasible [74,75], resulting in methanol's dissolution in biodiesel.

Biodiesel contains large carbon–hydrogen chains (C + H), which exhibit significant similarity to the hydrocarbons of MGO [75], a fact that accounts for the easy solubility of biodiesel in MGO.

The process executed for the chemical mobility phenomenon involves the binding of methanol molecules with biodiesel's carboxyl groups, followed by the entire dissolution of biodiesel molecules into the MGO's hydrocarbon molecules, which are present in higher concentration in the mixture, based on the solvent–solute relationship.

The increase in temperature to which the mixture is subjected contributes to a reduction in the cohesive bonds of methanol molecules, facilitating the dissolution phenomenon [75].

The spectrometry of the final mixture confirms the presence of the three utilized materials without the presence of an emulsifying additive, which verifies that mixing occurred via the aforementioned procedure, as shown in Figure 9 below.
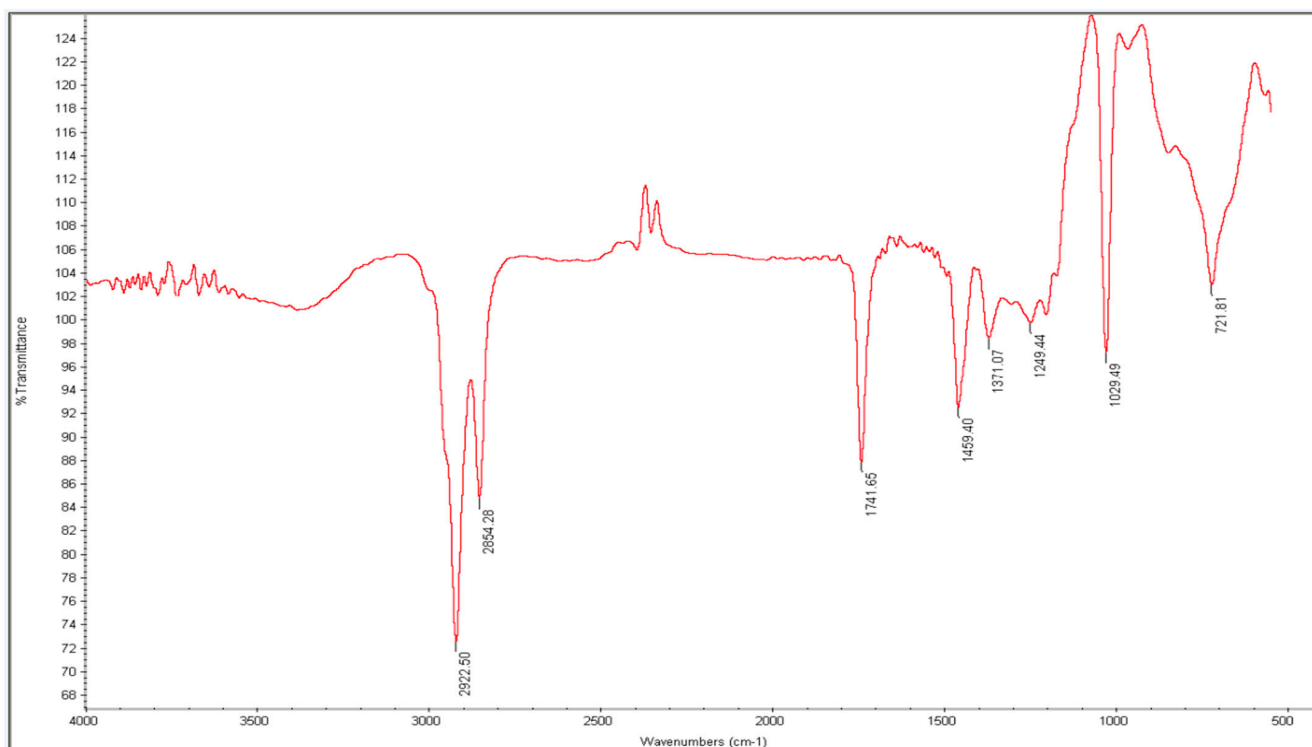
FT-IR

Figure 9. Final blend's spectrometry.

The spectrometry was conducted with an Agilent brand device, model FTIR Cary 630, made in the USA, in a spectral range of KBr 7000–350cm^{-1}, ZnSe 5100–600cm^{-1}, with spectral resolution < 2 cm^{-1}, wavenumber accuracy 0.05 cm^{-1} measured with the ASTM 1921 [76] method, and wavenumber reproducibility 0.005 cm^{-1} measured with the ASTM 1921 method.

The final mixture exhibits characteristics similar to conventional MGO, as shown in the Table 12 below; however, reduced viscosity was observed, albeit within the limits specified by ISO 8217:2017 [73], and at a lower calorific value. The comparison table is shown below.

Table 12. Comparison of final blend and conventional fuel.

Parameter	Final Blend's Measurement	Conventional Fuel's Measurement
Density	0.8423 gr/mL	0.8353 gr/mL
Kinematic Viscosity (40 °C)	2.9319 cSt	2.9912 cSt
Heat-producing Energy	38,746 J/gr	45,919 J/gr
Sulfur (S)	0.0104% *w/w*	0.090 *w/w*
HC Containing C$_{10}$–C$_{40}$	34.2% *w/w*	94% *w/w*
MeOH Content	20.2% *w/w*	00.0 *w/w*
Electrical Conductivity	>2000 pS	3 pS

The low viscosity is a factor that may confirm the need for modification of marine engines.

The lower calorific value is not a fuel's negative factor, as ultimately its energy efficiency is not reduced due to the increased number of ketones contained in the biodiesel.

The most significant drawback from the measurements so far arises in the indication of the increased electrical conductivity value, which appears to be attributed to the presence of water in the biodiesel and methanol.

The reduced fuel's carbon and sulfur content leads to a decrease in carbon dioxide and sulfur oxides emissions into the atmosphere, contributing to the reduction in factors responsible for the greenhouse effect and ensuring global health. A further study is already underway to accurately measure the emissions resulting from the use of fuel.

By improving this method and the resulting material through the continuous advancement of our research, we will be able to utilize a unified methanol fuel mixture without the need for dual-fuel engines, achieving reduced SO$_x$ and CO$_2$ emissions. This is because the emissions are proportional to the carbon and sulfur content of the fuel.

Further research will focus on the fuel's burning in marine engines and studying methods to reduce the fuel's electrical conductivity, as well as on finding new techniques for maintaining the fuel at even lower temperatures.

5. Conclusions

In summary, the continuously conventional fossil fuels' use increasing by shipping, has led to a hazardous gas emissions' rise, responsible for the greenhouse effect and global warming, while also creating conditions hazardous to global health. This phenomenon has entered the international organizations' agenda for the implementation of measures to reduce ships' gas emissions.

Among other measures, strict limits have been set on the fuels' sulfur content with the aim of their complete phase-out by 2050, while efforts are also being made to reduce carbon dioxide emissions by 50% during the same period. Measures implemented so far to comply with these regulations include modifying conventional fuels or developing new eco-friendly fuels. Significant alternatives include alcohols primarily used as additives to conventional fuel and biofuels. Methanol represents the cleanest alcohol with only one carbon atom in its molecule while being sulfur-free. However, its use in a blend with MGO is deemed impractical without the addition of costly additives. Nevertheless, through the experimental process of this study, the possibility of blending methanol with marine gas oil (MGO) with characteristics akin to conventional fuel is demonstrated, utilizing exclusively animal-derived biodiesel (FAME) as a blending aid under specific temperature conditions.

The maximum blending ratio of methanol—animal biodiesel (FAME)—marine fuel is 21.5% *v/v*–43% *v/v*–35.5% *v/v* respectively, by a method that requires prolonged uniform mixture's heating exposure, following by materials' separate heating. As a result of this method, the final product presents a C_{10}–C_{40} hydrocarbons' content decreased minimally, with a retention of 34.2% compared to the initial quantity corresponding to 35.5%. Methanol also decreased slightly, with a content of 20.2% of the initial quantity corresponding to 21% *v/v* of the mixture and the sulfur content remains almost negligible, at a rate of 0.0104% *w/w* of the initial mixture.

Additionally, the final blend meets the conventional fuel's properties with a calorific value reaching 38,746 J/g, the density (d) reaching at 0.8423 g/mL, and the kinematic viscosity at 40 °C the 2.9319 cSt.

6. Patents

For the final methodology and the produced material, patent number 1010615 has been granted by the Industrial Property Organization, with International Classification (INT. Cl. 2023.01): C10L 1/14, C10L 1/04, C10L 1/18, C10L 10/00, to the inventor, author, and corresponding author of the present paper, Mr. Dimitrios Parris.

Author Contributions: Conceptualization, D.P., K.S. and C.T.; methodology, D.P.; validation, D.P., K.S., K.P. and C.T.; formal analysis, D.P.; investigation, D.P., K.S. and K.P.; resources, D.P., K.S. and C.T.; data curation, D.P. and K.S; writing—original draft preparation, D.P.; writing—review and editing, D.P., K.S. and K.P.; visualization, K.S., K.P. and C.T.; supervision, K.S., K.P. and C.T.; project administration, D.P., K.S. and C.T. All authors have read and agreed to the published version of the manuscript.

Institutional Review Board Statement: Not applicable.

Informed Consent Statement: Not applicable.

Data Availability Statement: All data are available by corresponding author.

Conflicts of Interest: The authors declare no conflicts of interest.

Appendix A

Table A1. Physical properties of methanol [71].

Standard Physicochemical Properties	Liquid Properties
Melting point: −97.7 °C	Density: 791 kg/m^3 at 20 °C
Boiling point: 64.9 °C	Heat of vaporization: 35,278 kJ/kmol
Relative density: 0.79	Viscosity:
Formula: CH_3OH	a = 555.3 b = 260.6
Molecular weight: 32.042 kg/kmol	where log(viscosity) = a * (1/T − 1/b)
Heat of formation: −201.3 MJ/kmol	Viscosity: mNs/m² T: °K
Gibbs free energy: −162.62 MJ/kmol	**Vapor Properties**
Freezing point: −97.7 °C	Heat capacity:
Boiling point: 64.6 °C (at atmospheric pressure)	a = 21.152 b = 0.07092 c = 2.59×10^{-5} d = -2.85×10^{-8}, where Cp = a + b * T + c * T^2 + d * T^3 Cp: kmol.K T: °K
Critical properties	**Vapor pressure**
Critical temperature: 512.6 K	a = 18.5875 b = 3626.55 c = −34.29
Critical pressure: 81 bar abs	where ln(P) = a − b/(T + c) P: mmHg; T: °K within range −16 to 91 °C
Critical volume: 0.118 m^3/kmol	

Table A2. Animal biodiesel specs.

Parameter	Units	Minimum Allowable	Maximum Allowable
Ester	% (w/w)	96.0	
Density @ 15 °C	kg/m^3	860.0	900.0
Viscosity @ 40 °C	mm^2/s	3.50	5.00
Flame point	°C	120.0	
Sulfur	mg/kg		10.0
Carbon residue	% (w/w)		0.30
Cctanc number	-	51.0	
Sulfated ash	% (w/w)		0.02
Moisture	mg/kg		500.0
Total contamination	mg/kg		24.0
Corrosion to copper	-	Class 1	
Oxidation stability @ 110 °C	h	6.0	
Acidity index	mg KOH/g		0.50
Iodine index	g I$_2$/100 g		120.0
Methyl ester of linolcic acid	% (w/w)		12.0
Poly unsaturated methyl esters	% (w/w)		1.0
Methanol	% (w/w)		0.20
Monoglyccridcs	% (w/w)		0.90
Diglyccridcs	% (w/w)		0.20
Triglycerides	% (w/w)		0.20
Free glycerol	% (w/w)		0.02
Total glycerol	% (w/w)		0.25
Group I metals (Na+K.)	mg/kg		5.0
Group II metals (Ca+Mg)	mg/kg		5.0
Stability limit temperature	°C	Contractual values	
Phosphorus	mg/kg		10.0

Table A3. Marine distillate fuel standards [73].

Limit	Parameter	DMX	DMA	DFA	DMZ	DFZ	DMB	DFB
Max.	Viscosity at 40 °C (mm^2/s) (1 mm^2/s = 1 cSt)	5.500	6.000		6.000		11.00	
Min.	Viscosity at 40 °C (mm^2/s)	1.400	2.000		3.000		2.000	
Max.	Micro carbon residue at 10% residue (% m/m)	0.30	0.30		0.30		-	
Max.	Density at 15 °C (kg/m^3)	-	890.0		890.0		900.0	
Max.	Micro carbon residue (% m/m)	-	-		-		0.30	
Max.	Sulfur (% m/m)	1.00	1.00		1.00		1.50	
Max.	Water (% v/v)	-	-		-		0.30	
Max.	Total sediment by hot filtration (% m/m)	-	-		-		0.10	
Max.	Ash (% m/m)	0.010	0.010		0.010		0.010	
Min.	Flash point (°C)	43.0	60.0		60.0		60.0	
Max.	Pour point in winter (°C)	-	−6		−6		0	
Max.	Pour point in summer (°C)	-	0		0		6	
Max.	Cloud point in winter (°C)	−16	Report		Report		-	
Max.	Cloud point in summer (°C)	−16	-		-		-	
Max.	Cold filter plugging point in winter (°C)	-	Report		Report		-	
Max.	Cold filter plugging point in summer (°C)	-	-		-		-	
Min.	Calculated cetane index	45	40		40		35	
Max.	Acid number (mgKOH/g)	0.5	0.5		0.5		0.5	
Max.	Oxidation stability (g/m^3)	25	25		25		25	
Max.	Fatty acid methyl ester (FAME)	-	-	7.0	-	7.0	-	7.0
Max.	Lubricity, corrected wear scar diameter (wsd 1.4 at 60 °C) (μm)	520	520		520		520	
Max.	Hydrogen sulfide (mg/kg)	2.00	2.00		2.00		2.00	
	Appearance	Clear and bright					-	

References

1. Xing, H.; Spence, S.; Chen, H. A Comprehensive Review on Countermeasures for CO_2 Emissions from Ships. *Renew. Sustain. Energy Rev.* **2020**, *134*, 110222. [CrossRef]
2. Bortnowska, M. Projected Reductions in CO_2 Emissions by Using Alternative Methanol Fuel to Power a Service Operation Vessel. *Energies* **2023**, *16*, 7419. [CrossRef]
3. Walker, T.R.; Adebambo, O.; Del Aguila Feijoo, M.C.; Elhaimer, E.; Hossain, T.; Edwards, S.J.; Morrison, C.E.; Romo, J.; Sharma, N.; Taylor, S. Environmental Effects of Marine Transportation. In *World Seas: An Environmental Evaluation*; Elsevier: Amsterdam, The Netherlands, 2019; pp. 505–530.
4. Tomos, B.A.D.; Stamford, L.; Welfle, A.; Larkin, A. Decarbonising International Shipping—A Life Cycle Perspective on Alternative Fuel Options. *Energy Convers. Manag.* **2024**, *299*, 117848. [CrossRef]
5. WTO. International Trade Statistics. Available online: https://www.wto.org/english/res_e/statis_e/statis_e.htm (accessed on 28 June 2024).
6. IEA. *Transportation Sector Energy Consumption*; IEA: Paris, France, 2016.
7. Parris, D.; Spinthiropoulos, K.; Ragazou, K.; Giovou, A.; Tsanaktsidis, C. Methanol, a Plugin Marine Fuel for Green House Gas Reduction—A Review. *Energies* **2024**, *17*, 605. [CrossRef]
8. Eyring, V.; Isaksen, I.S.A.; Berntsen, T.; Collins, W.J.; Corbett, J.J.; Endresen, O.; Grainger, R.G.; Moldanova, J.; Schlager, H.; Stevenson, D.S. Transport Impacts on Atmosphere and Climate: Shipping. *Atmos. Environ.* **2010**, *44*, 4735–4771. [CrossRef]
9. Aakko-Saksa, P.T.; Lehtoranta, K.; Kuittinen, N.; Järvinen, A.; Jalkanen, J.-P.; Johnson, K.; Jung, H.; Ntziachristos, L.; Gagné, S.; Takahashi, C.; et al. Reduction in Greenhouse Gas and Other Emissions from Ship Engines: Current Trends and Future Options. *Prog. Energy Combust. Sci.* **2023**, *94*, 101055. [CrossRef]
10. Fayyazbakhsh, A.; Bell, M.L.; Zhu, X.; Mei, X.; Koutný, M.; Hajinajaf, N.; Zhang, Y. Engine Emissions with Air Pollutants and Greenhouse Gases and Their Control Technologies. *J. Clean. Prod.* **2022**, *376*, 134260. [CrossRef]
11. Singh, S.K.; Chauhan, A.; Sarkar, B. Strategy Planning for Sustainable Biodiesel Supply Chain Produced from Waste Animal Fat. *Sustain. Prod. Consum.* **2024**, *44*, 263–281. [CrossRef]
12. Olmer, N.; Olmer, C.; Roy, B.; Mao, X.; Rutherford, D. *Greenhouse Gas Emissions from Global Shipping, 2013–2015 Detailed Methodology*; International Council on Clean Transportation: Washington, DC, USA, 2017; pp. 1–38.
13. ABS. *Setting the Course to Low Carbon Shipping*; ABS: Houston, TX, USA, 2019.
14. Urban, F.; Nurdiawati, A.; Harahap, F. Sector Coupling for Decarbonization and Sustainable Energy Transitions in Maritime Shipping in Sweden. *Energy Res. Soc. Sci.* **2024**, *107*, 103366. [CrossRef]
15. EMSA. CO_2 *Emission Report*; EMSA: Lisbon, Portugal, 2023.
16. Krantz, G.; Brandao, M.; Hedenqvist, M.; Nilsson, F. Indirect CO_2 Emissions Caused by the Fuel Demand Switch in International Shipping. *Transp. Res. Part D Transp. Environ.* **2022**, *102*, 103164. [CrossRef]
17. Mason, J.; Larkin, A.; Gallego-Schmid, A. Mitigating Stochastic Uncertainty from Weather Routing for Ships with Wind Propulsion. *Ocean Eng.* **2023**, *281*, 114674. [CrossRef]
18. Du, W.; Li, Y.; Zhang, G.; Wang, C.; Zhu, B.; Qiao, J. Energy Saving Method for Ship Weather Routing Optimization. *Ocean Eng.* **2022**, *258*, 111771. [CrossRef]
19. Farkas, A.; Degiuli, N.; Martić, I.; Mikulić, A. Benefits of Slow Steaming in Realistic Sailing Conditions along Different Sailing Routes. *Ocean Eng.* **2023**, *275*, 114143. [CrossRef]
20. Balcombe, P.; Brierley, J.; Lewis, C.; Skatvedt, L.; Speirs, J.; Hawkes, A.; Staffell, I. How to Decarbonise International Shipping: Options for Fuels, Technologies and Policies. *Energy Convers. Manag.* **2019**, *182*, 72–88. [CrossRef]
21. Rivarolo, M.; Rattazzi, D.; Magistri, L.; Massardo, A.F. Multi-Criteria Comparison of Power Generation and Fuel Storage Solutions for Maritime Application. *Energy Convers. Manag.* **2021**, *244*, 114506. [CrossRef]
22. Mallouppas, G.; Yfantis, E.A. Decarbonization in Shipping Industry: A Review of Research, Technology Development, and Innovation Proposals. *J. Mar. Sci. Eng.* **2021**, *9*, 415. [CrossRef]
23. The European Parliament and the Council of the European Union Directive (EU) 2016/802 of the European Parliament and of the Council of 11 May 2016 Relating to a Reduction in the Sulphur Content of Certain Liquid Fuels (Codification). Available online: https://eur-lex.europa.eu/legal-content/en/ALL/?uri=CELEX:32016L0802 (accessed on 28 June 2024).
24. Ma, S.; Guo, Q.; Wei, J.; Yin, Z.; Zhuang, Y.; Zhang, Y.; Dai, Q.; Qian, Y. Analyzing the Effect of Carbon Nanoparticles on the Combustion Performance and Emissions of a DI Diesel Engine Fueled with the Diesel-Methanol Blend. *Energy* **2024**, *300*, 131616. [CrossRef]
25. Tian, Z.; Wang, Y.; Zhen, X.; Liu, Z. The Effect of Methanol Production and Application in Internal Combustion Engines on Emissions in the Context of Carbon Neutrality: A Review. *Fuel* **2022**, *320*, 123902. [CrossRef]
26. Kanchiralla, F.M.; Brynolf, S.; Malmgren, E.; Hansson, J.; Grahn, M. Life-Cycle Assessment and Costing of Fuels and Propulsion Systems in Future Fossil-Free Shipping. *Environ. Sci. Technol.* **2022**, *56*, 12517–12531. [CrossRef]
27. Methanol Institute. Renewable Methanol. Available online: https://www.methanol.org/renewable/ (accessed on 28 June 2024).
28. Duraisamy, G.; Rangasamy, M.; Govindan, N. A Comparative Study on Methanol/Diesel and Methanol/PODE Dual Fuel RCCI Combustion in an Automotive Diesel Engine. *Renew. Energy* **2020**, *145*, 542–556. [CrossRef]
29. Huang, J.; Fan, H.; Xu, X.; Liu, Z. Life Cycle Greenhouse Gas Emission Assessment for Using Alternative Marine Fuels: A Very Large Crude Carrier (VLCC) Case Study. *J. Mar. Sci. Eng.* **2022**, *10*, 1969. [CrossRef]

30. Balcombe, P.; Staffell, I.; Kerdan, I.G.; Speirs, J.F.; Brandon, N.P.; Hawkes, A.D. How Can LNG-Fuelled Ships Meet Decarbonisation Targets? An Environmental and Economic Analysis. *Energy* **2021**, *227*, 120462. [CrossRef]

31. Andersson, K.; Salazar, C.M. *Methanol as a Marine Fuel Report*; FCBI Energy: London, UK, 2015; pp. 1–46.

32. Grijpma, P. *Sustainable Marine Biofuel for the Dutch Bunker Sector*; Utrecht University: Utrecht, The Netherlands, 2018.

33. Karabektas, M.; Ergen, G.; Hosoz, M. Effects of the Blends Containing Low Ratios of Alternative Fuels on the Performance and Emission Characteristics of a Diesel Engine. *Fuel* **2013**, *112*, 537–541. [CrossRef]

34. Ellis, J.; Tanneberger, K. *Study on the Use of Ethyl and Methyl Alcohol as Alternative Fuels in Shipping*; European Maritime Safety Agency: Lisbon, Portugal, 2015; pp. 1–38.

35. Hellström, M.; Rabetino, R.; Schwartz, H.; Tsvetkova, A.; Haq, S.H.U. GHG Emission Reduction Measures and Alternative Fuels in Different Shipping Segments and Time Horizons—A Delphi Study. *Mar. Policy* **2024**, *160*, 105997. [CrossRef]

36. Gaurav, N.; Sivasankari, S.; Kiran, G.; Ninawe, A.; Selvin, J. Utilization of Bioresources for Sustainable Biofuels: A Review. *Renew. Sustain. Energy Rev.* **2017**, *73*, 205–214. [CrossRef]

37. Varma, P.; Otageri, J.; Kandasubramanian, B. Biodiesel from Fats: Fatty Acid Feedstock as a Circular Economy Solution. *Int. J. Green Energy* **2024**, 1–21. [CrossRef]

38. Shahir, V.K.; Jawahar, C.P.; Suresh, P.R. Comparative Study of Diesel and Biodiesel on CI Engine with Emphasis to Emissions—A Review. *Renew. Sustain. Energy Rev.* **2015**, *45*, 686–697. [CrossRef]

39. Kumar, N.; Varun; Chauhan, S.R. Performance and Emission Characteristics of Biodiesel from Different Origins: A Review. *Renew. Sustain. Energy Rev.* **2013**, *21*, 633–658. [CrossRef]

40. Kongprawes, G.; Wongsawaeng, D.; Hosemann, P.; Ngaosuwan, K.; Kiatkittipong, W.; Assabumrungrat, S. Dielectric Barrier Discharge Plasma for Catalytic-Free Palm Oil Hydrogenation Using Glycerol as Hydrogen Donor for Further Production of Hydrogenated Fatty Acid Methyl Ester (H-FAME). *J. Clean. Prod.* **2023**, *401*, 136724. [CrossRef]

41. Mohd Noor, C.W.; Noor, M.M.; Mamat, R. Biodiesel as Alternative Fuel for Marine Diesel Engine Applications: A Review. *Renew. Sustain. Energy Rev.* **2018**, *94*, 127–142. [CrossRef]

42. Babazadeh, R. Application of Fuzzy Optimization to Bioenergy-Supply-Chain Planning under Epistemic Uncertainty: A New Approach. *Ind. Eng. Chem. Res.* **2019**, *58*, 6519–6536. [CrossRef]

43. Banković-Ilić, I.B.; Stojković, I.J.; Stamenković, O.S.; Veljkovic, V.B.; Hung, Y.-T. Waste Animal Fats as Feedstocks for Biodiesel Production. *Renew. Sustain. Energy Rev.* **2014**, *32*, 238–254. [CrossRef]

44. Habib, M.S.; Tayyab, M.; Zahoor, S.; Sarkar, B. Management of Animal Fat-Based Biodiesel Supply Chain under the Paradigm of Sustainability. *Energy Convers. Manag.* **2020**, *225*, 113345. [CrossRef]

45. Wan Omar, W.N.N.; Saidina Amin, N.A. Optimization of Heterogeneous Biodiesel Production from Waste Cooking Palm Oil via Response Surface Methodology. *Biomass Bioenergy* **2011**, *35*, 1329–1338. [CrossRef]

46. Tan, K.T.; Lee, K.T.; Mohamed, A.R. Potential of Waste Palm Cooking Oil for Catalyst-Free Biodiesel Production. *Energy* **2011**, *36*, 2085–2088. [CrossRef]

47. Demirbas, A. Progress and Recent Trends in Biodiesel Fuels. *Energy Convers. Manag.* **2009**, *50*, 14–34. [CrossRef]

48. Yaakob, Z.; Mohammad, M.; Alherbawi, M.; Alam, Z.; Sopian, K. Overview of the Production of Biodiesel from Waste Cooking Oil. *Renew. Sustain. Energy Rev.* **2013**, *18*, 184–193. [CrossRef]

49. Freedman, B.; Pryde, E.H.; Mounts, T.L. Variables Affecting the Yields of Fatty Esters from Transesterified Vegetable Oils. *J. Am. Oil Chem. Soc.* **1984**, *61*, 1638–1643. [CrossRef]

50. Ma, F.; Hanna, M.A. Biodiesel Production: A review1Journal Series #12109, Agricultural Research Division, Institute of Agriculture and Natural Resources, University of Nebraska–Lincoln.1. *Bioresour. Technol.* **1999**, *70*, 1–15. [CrossRef]

51. Wang, Y.; Ou, S.; Liu, P.; Xue, F.; Tang, S. Comparison of Two Different Processes to Synthesize Biodiesel by Waste Cooking Oil. *J. Mol. Catal. A Chem.* **2006**, *252*, 107–112. [CrossRef]

52. Mittelbach, M.; Enzelsberger, H. Transesterification of Heated Rapeseed Oil for Extending Diesel Fuel. *J. Am. Oil Chem. Soc.* **1999**, *76*, 545–550. [CrossRef]

53. Sharma, Y.C.; Singh, B. Development of Biodiesel from Karanja, a Tree Found in Rural India. *Fuel* **2008**, *87*, 1740–1742. [CrossRef]

54. Dizge, N.; Aydiner, C.; Imer, D.Y.; Bayramoglu, M.; Tanriseven, A.; Keskinler, B. Biodiesel Production from Sunflower, Soybean, and Waste Cooking Oils by Transesterification Using Lipase Immobilized onto a Novel Microporous Polymer. *Bioresour. Technol.* **2009**, *100*, 1983–1991. [CrossRef] [PubMed]

55. Feng, H.; Chen, X.; Sun, L.; Ma, R.; Zhang, X.; Zhu, L.; Yang, C. The Effect of Methanol/Diesel Fuel Blends with Co-Solvent on Diesel Engine Combustion Based on Experiment and Exergy Analysis. *Energy* **2023**, *282*, 128792. [CrossRef]

56. Vargün, M.; Turgut Yılmaz, I.; Sayın, C. Investigation of Performance, Combustion and Emission Characteristics in a Diesel Engine Fueled with Methanol/Ethanol/nHeptane/Diesel Blends. *Energy* **2022**, *257*, 124740. [CrossRef]

57. Paulauskiene, T.; Bucas, M.; Laukinaite, A. Alternative Fuels for Marine Applications: Biomethanol-Biodiesel-Diesel Blends. *Fuel* **2019**, *248*, 161–167. [CrossRef]

58. SR EN ISO 20884. Standard Test Methods for Petroleum products—Determination of Sulfur Content of Automotive Fuels—Wavelength-Dispersive X-ray Fluorescence Spectrometry. Available online: https://standards.iteh.ai/catalog/standards/cen/2156a459-967a-46dc-9f39-84ec125456ba/en-iso-20884-2019 (accessed on 28 June 2024).

59. *EN ISO 12185:1996*; Petroleum Products—Determination of Density—Oscillating U-Tube Method. International Organization for Standardization ISO: Geneva, Switzerland, 1996.

60. *EN ISO 3104:2020*; Petroleum Products—Transparent and Opaque Liquids—Determination of Kinematic Viscosity and Calculation of Dynamic Viscosity. International Organization for Standardization ISO: Geneva, Switzerland, 2020.
61. ASTM D240-19. Available online: https://cdn.standards.iteh.ai/samples/104736/63404a2a7ef44099b2848e3933d04f6e/ASTM-D240-19.pdf (accessed on 28 June 2024).
62. ISO 17025:2017. Available online: https://www.iasonline.org/wp-content/uploads/2021/02/ISO-IEC-17025-2017-IAS.pdf (accessed on 28 June 2024).
63. *ASTM D2624*; Standard Test Methods for Electrical Conductivity of Aviation and Distillate Fuels. American Society for Testing and Materials International: West Conshohocken, PA, USA, 2009.
64. EVS-EN ISO 20846:2011. Petroleum Products—Determination of Sulfur Content of Automotive Fuels—Ultraviolet Fluorescence Method. Available online: https://www.evs.ee/tooted/evs-en-iso-20846-2011 (accessed on 28 June 2024).
65. EN ISO 3679. Available online: https://www.iso.org/obp/ui/#iso:std:iso:3679:ed-5:v1:en (accessed on 28 June 2024).
66. EN 23015. Available online: https://standards.iteh.ai/catalog/standards/cen/616161ad-c21a-4355-8482-0a4f1dae8a47/en-23015-1994 (accessed on 28 June 2024).
67. EN ISO 12937. Available online: https://www.iso.org/obp/ui/#iso:std:iso:12937:ed-1:v1:en (accessed on 28 June 2024).
68. EN 14104. Available online: https://www.en-standard.eu/bs-en-14104-2021-fat-and-oil-derivates-fatty-acid-methyl-ester-fame-determination-of-acid-value/?gad_source=1&gclid=Cj0KCQjw5ea1BhC6ARIsAEOG5pz3v2pUVBzcThKUfTnHcqsJGK5py_VR4FGMYYDx5ONojTPnMq4Nf7kaAg9oEALw_wcB (accessed on 28 June 2024).
69. EN 14103. Available online: https://standards.iteh.ai/catalog/standards/cen/2eb3696f-7f13-49f2-846e-0ebd8f4c42ea/en-14103-2020 (accessed on 28 June 2024).
70. EN 15779. Available online: https://standards.iteh.ai/catalog/standards/cen/7a67c5ae-188b-4ef8-97d6-6dc7ba1f6396/en-15779-2009a1-2013 (accessed on 28 June 2024).
71. Cetiner Engineering Corporation. Methanol Physical Properties. Available online: https://www.cetinerengineering.com/Properties.htm (accessed on 28 June 2024).
72. EN 14214. Available online: https://standards.iteh.ai/catalog/standards/cen/0a2c5899-c226-479c-b277-5322cc71395d/en-14214-2012a2-2019 (accessed on 28 June 2024).
73. *ISO 8217:2017*; Petroleum Products Fuels (Class F) Specifications of Marine Fuels. ISO: Geneva, Switzerland, 2012.
74. Morrison, R.T.; Boyd, R.N. *Organic Chemistry*, 6th ed.; Prentice Hall: Englewood Cliffs, NJ, USA, 2006; ISBN 978-0-13-643669-0.
75. Tsanaktsidis, C.G. Optimizing the Physical–Chemical Properties of Diesel Fuel by Introducing Bio-Organic Compounds. *Chem. Technol. Fuels Oils* **2011**, *47*, 209–212. [CrossRef]
76. ASTM 1921. Available online: https://www.nist.gov/system/files/documents/srm/SP260-122.pdf (accessed on 28 June 2024).